Journal of Sound and Vibration 432 (2018) 420–436

Contents lists available at ScienceDirect

Journal of Sound and Vibration

journal homepage: www.elsevier.com/locate/jsvi

Dynamics and optimal control of an electromagnetically actuated cantilever pipe conveying fluid

Dominik Pisarski, Robert Konowrocki, Tomasz Szmidt *

Institute of Fundamental Technological Research, Polish Academy of Sciences, Pawińskiego 5B, 02-106 Warsaw, Poland

ARTICLE INFO

Article history:
Received 7 September 2017
Revised 14 May 2018
Accepted 18 June 2018
Available online XXX
Handling Editor: J. Lam

Keywords:
Fluid–structure interaction
Electromagnetic device
Optimal control
Stabilization
Smart structure

ABSTRACT

This paper deals with the problem of applying electromagnetic devices of the motional type to improve the dynamic stability of a pipe conveying air. When the flow velocity reaches a critical value, the steady equilibrium position becomes unstable, and self-excited lateral vibrations arise. In contrast, electromagnetic devices of the transformer type have been demonstrated to be highly effective in the passive stabilization of such a system, as well as the active stabilization of similar non-conservative systems with a follower force. In the present paper, we apply a pair of motional devices made of a conducting plate which is attached to the pipe and moves together with it within the perpendicular magnetic field generated by the controlled electromagnets. This motion generates eddy currents in the plates and a drag force of a viscous character. In this setting, we first investigate the possibility of designing a stabilizing control within the region of the magnetic field where every passive solution results in an unstable or conservative state. For that purpose, we determine a practical condition justifying the existence of a stabilizing control for a given set of system parameters. Later we pose and solve an optimal control problem aiming at stabilizing the system with the optimal rate of decrease of the system's energy. The solution is examined by means of numerical simulations performed within the three regions of the flow velocity: low subcritical, where the Coriolis acceleration of the conveyed fluid generates the predominate damping force; high subcritical, where the inertia of the fluid begins to dominate the dynamics of the system; and low supercritical, where unstable flutter vibrations start to arise. The effectiveness of the designed optimal controller is validated by comparisons with the corresponding passive solutions.

1. Introduction

Since the first half of the twentieth century, pipes conveying fluid have attracted much the subject of much research [1]. The reasons for this include not only the practical importance of the problem itself, but also gathering knowledge useful in other areas of fluid–structure interactions [2]. Moreover, cantilever pipes with flow are one of the few examples in engineering applications of a non-conservative elastic system subjected to a follower force, i.e., a force that always remains tangential to the deflected axis of the slender structure [3]. When the flow velocity becomes sufficiently high, self-excited flutter vibrations arise, unlike the case of pipes supported at both ends, which are prone to a buckling type of instability [4]. This can be easily observed when a strong stream of water starts flowing inside a garden hose: its free end begins a snake-like motion on the grass. Such systems are extremely susceptible to changes in the physical parameters and to the introduction of new effects. Even the simple

* Corresponding author.
E-mail address: tszmidt@ippt.pan.pl (T. Szmidt).

https://doi.org/10.1016/j.jsv.2018.06.045

effect of a viscous-type damping or an additional lumped mass can decrease the critical flow velocity or stabilize the system, depending on the values of its parameters [5,6].

The aforementioned article of Imbrahim [1] lists over 30 research papers related to the control of fluid-conveying pipes. Almost all of them describe the concept of generating transverse forces or bending moments acting on the system in an active way, depending on the system's state, within a closed feedback loop. For this various actuators have been used. Examples include servomotors connected to a pipe via tendons or springs [7–9], gyroscopic mechanisms [10], and piezoelectric elements mounted on a pipe [11,12] or embedded in its material [13]. In some of these papers, the type of actuator is not defined, aiming at more general results, for example the simultaneous optimization of the pipe's shape and the actuators' position [14] or exploring the possibility of applying a reduced model for active nodal vibration control [15].

A drawback of active methods is the possibility of destabilizing the system if a failure happens, because the action of external forces or moments can introduce additional energy into the system (here, the system refers to the pipe and the fluid volume enclosed within it). In the present paper, we propose the use of a semi-active method based on an electromechanical eddy-current damper of the motional (Lorentz) type. In various structural control applications, the employment of the semi-active devices verified a favorable balance between the performance and robustness [16–20] while reducing the amount of consumed energy compared to the active actuators. Electromechanical dampers of the motional type are reported to be usually more effective than the dampers of the other widely used category, namely, the transformer devices [21,22], which exhibited mediocre performance when used for passive stabilization of a fluid-conveying pipe [23]. In its simplest form, the motional damper consists of a conducting plate which moves within a perpendicular and constant magnetic field, as for example in an analogue electricity meter. This motion generates eddy currents in the plate and a drag force, which is a consequence of the Lenz law. Due to the constant value of the magnetic flux, the damping force depends linearly on the plate's velocity, and thus these dampers act as viscous ones, with a damping coefficient depending on the geometry of the plate and the magnetic flux [24].

Motional dampers were considered for use in vehicle suspension systems [25] as well as for reducing the lateral vibrations of a rotating shaft [26]. Such actuators are contact-free, so they do not disturb the pipe, apart from introducing an additional mass. Moreover, they allow an easy implementation of a control strategy by appropriate changes of the magnetic field.

Another key feature of our approach is an open-loop scheme. In the majority of the literature referred to above, closed-loop control schemes are employed. An observation of the system's state is necessary if it undergoes a complicated motion, such as, the chaotic vibrations which may occur if a pipe is subjected to non-linear constraints [27]. It is also known that pipes with flow and added mass or even plain pipes may lose the stability with a rich variety of bifurcations, including a 3-d chaotic motion or jump phenomena [28–32], depending on the system's parameters. However, in our case, we deal with periodic, thus predictable, both free and self-excited vibrations, which is guaranteed by the relevant selection of the parameters (see Section 2.2).

In the control design, we shall focus on stabilizing the vibrations of the pipe while respecting the constraints imposed by the physical properties of the electromechanical damper employed. First, we will examine the existence of stabilizing controls operating within the input range where any passive solution results in conservative or unstable dynamics. Then, we will propose a controller relying on the solution to a constrained bilinear optimal control problem. The numerical algorithm for solving the optimization problem will be given and examined for convergence. The performance of the designed control will be validated by means of numerical simulations. We will investigate several scenarios for a range of flow velocity and different placements of the actuator.

The remainder of this paper is structured as follows. Section 2 introduces the mathematical model of the fluid-conveying pipe actuated by the electromechanical damper. In Section 3, we derive a discrete representation of the investigated system. The fundamental dynamical properties of the examined structure are studied in Section 4. In Section 5, the optimal stabilization problem is formulated and the method of solution is presented. In Section 6, the performance of the designed control method is validated by means of numerical simulations. Some conclusions and avenues for future research are provided in Section 7.

2. The examined system

2.1. The equations of motion

We are going to study the dynamics of a standing cantilevered pipe conveying a fluid, with motional-type electromagnetic devices attached to it, see Fig. 1. The pipe is slender, and small transverse vibrations in the plane of symmetry $\xi - w$ are considered, so the linear Bernoulli–Euler theory can be applied. The horizontal deflection of the pipe is denoted by $w = w(\xi, t)$. A viscous-type internal damping is present. Gravity is taken into account and acts vertically downwards. The mass of the conducting plates that are part of the actuators is incorporated in a lumped form, but their rotatory inertia is neglected. We employ the plug flow model, i.e., we assume that the flow velocity is constant across every cross-section perpendicular to the pipe's longitudinal axis.

Under the above assumptions, the governing equation of the pipe's motion takes the form

$$\begin{aligned} &EI\frac{\partial^4 w}{\partial \xi^4} + E^* I\frac{\partial^5 w}{\partial \xi^4\,\partial t} + \left[m_f v^2 + \left(m + m_f\right)(L-\xi)\,g + \mathbf{1}_{[0,\xi_a]} M_a g\right]\frac{\partial^2 w}{\partial \xi^2} + 2m_f v\frac{\partial^2 w}{\partial \xi\,\partial t} \\ &- \left(m + m_f + M_a\delta_a\right) g\frac{\partial w}{\partial \xi} + C\left(B_1^2 + B_2^2\right)\delta_a\frac{\partial w}{\partial t} + \left(m + m_f + M_a\delta_a\right)\frac{\partial^2 w}{\partial t^2} = 0, \end{aligned} \tag{1}$$

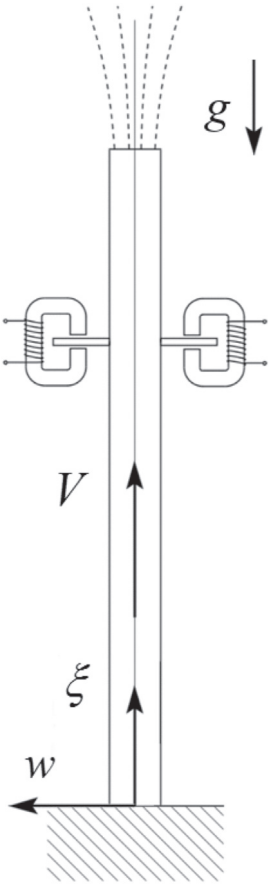

Fig. 1. Schematic of the examined system: Standing cantilever pipe conveying fluid together with electromagnetic devices of motional type.

where L denotes the length of the pipe, EI and E^*I the bending stiffness and damping of the pipe, m and m_f the masses of the pipe and the fluid per unit length, M_a the mass of the actuators attached to the pipe at the position ξ_a, v the flow velocity, C the constant of the viscous damping force generated by the electromagnetic actuators of motional type, B_1 and B_2 the magnetic inductions in the circuits of the actuators, g the acceleration due to gravity, δ_a is Dirac's delta function concentrated at ξ_a, and $\mathbf{1}_{[0,\xi_a]}$ is the indicator function of the interval $[0, \xi_a]$.

The boundary conditions correspond to the clamped support

$$w\Big|_{\xi=0} = \frac{\partial w}{\partial \xi}\Big|_{\xi=0} = \left(EI\frac{\partial^2 w}{\partial \xi^2} + E^*I\frac{\partial^3 w}{\partial \xi^2\,\partial t}\right)_{\xi=L} = \left(EI\frac{\partial^3 w}{\partial \xi^3} + E^*I\frac{\partial^4 w}{\partial \xi^3\,\partial t}\right)_{\xi=L} = 0. \tag{2}$$

Equation (1) is similar to the one validated in Ref. [33]. The only difference is an incorporation of internal dissipation in the pipe, which significantly affects the dynamics of the system and, obviously, the mass of the electromagnetic actuators and the drag force, whose influence is going to be studied. Note that the flutter can be described by four terms in this equation. Two of them are classical terms of a Bernoulli–Euler beam: the elastic restoring force and the inertia of the combined masses of the pipe and fluid. The other two are two opposite effects generated by the flow: the centrifugal force of the moving fluid $m_f v^2\,\partial^2 w/\partial \xi^2$, which destabilizes the system and may generate flutter vibrations, and the Coriolis force $2m_f v\,\partial^2 w/\partial \xi\,\partial t$, which exerts a damping effect.

The constant of viscous drag that appears in the term related to the electromagnetic devices was calculated by Bae et al. and is $C = \sigma h S\left(\alpha_1 + \alpha_2\right)$, where σ is the electric conductivity of the plate, h is the thickness of the plate, S is the cross-sectional area of the magnetic flux that passes perpendicularly through the plate (it is assumed that the flux remains within the area of the plate for the entire time of the vibrations), and α_1, α_2 are constants that depend on the geometry of the plate and the cross-section of the magnetic flux [24].

The proposed linear model of the system is valid providing that the real system exhibits periodic planar oscillations. This requires appropriate selection of the parameters, see Subsection 2.2.

Table 1
Parameters of the examined system.

Parameter	Unit	Value
Pipe length, L	m	0.965
Cross-sectional area, A	m^2	$13.35 \cdot 10^{-6}$
Cross-sectional moment of area, I	m^4	$1.21 \cdot 10^{-10}$
Young's modulus, E	$N\,m^{-2}$	$1.4 \cdot 10^{9}$
Internal damping coefficient, E^*	$N\,m^{-2}\,s$	$17.4 \cdot 10^{6}$
Pipe mass density, m	$kg\,m^{-1}$	0.01606
Fluid mass density, m_f	$kg\,m^{-1}$	0.00006
Mass of both actuators, M_a	kg	0.0321
Magnetic damping coefficient, C	$N\,s\,m^{-1}\,T^{-2}$	2.5926

2.2. Physical and geometrical parameters

We employ the parameters of the system taken from our preliminary experimental results on a test stand, which is currently under construction, see Table 1.

The pipe is made of ABS styrene, whose Young's modulus E and internal damping coefficient E^* were determined by us in a free-vibration test using typical commercially available tubes. The external and internal diameters are 0.009 and 0.008 m, respectively. We consider air as the moving fluid. An external damping exerts a stabilizing effect only if the mass density of the fluid m_f is sufficiently lower than the mass density of the pipe m; otherwise damping would decrease the critical flow velocity [5].

As for the electromagnetic devices, we assume each of the two plates attached to the pipe to be made of aluminum and to have dimensions $0.09 \times 0.04 \times 0.0015$ m. The cross-sections of both magnetic circuits are squares with size 0.01×0.01 m. The maximum induction that we consider amounts to $B_1 = B_2 = \sqrt{0.05} \approx 0.22$ T, which can be easily achieved in a magnetic circuit with a required gap of 0.006 m.

The selection of parameters is a compromise imposed by numerous limitations. It is well-known that pipes with flow may present a complex non-periodic or non-planar motion for flows beyond the critical value. Designing an optimal control for such systems is difficult. Thus we had to ensure that the flow velocity, mass of the of the fluid, pipe and actuators, and length of the pipe are such that the system exhibits periodic planar oscillations that can be captured by the linear model (1).

1. The considered flow velocities are below the critical value or slightly above it. If the flow velocity is sufficiently high then even a small mass attached at the end of the pipe brings a complex pattern of vibrations [30]
2. The mass ratio of the fluid and the pipe $\beta = m_f/(m_f + m)$ is appropriate. In certain ranges of this parameter the external damping actually destabilizes the pipe [5], whereas in other ranges the resultant post-critical vibrations are three-dimensional or non-periodic, even if the effect of an additional mass can be neglected [28,32].
3. The mass ratio of the actuators and the pipe $\Gamma = M_a/((m_f + m)L)$ is appropriate. The tip mass is known to yield a complex motion of the pipe, however for certain ranges of Γ and flows slightly exceeding the critical value the resultant bifurcation is planar and periodic [29,31].

Moreover, our idea was to obtain results that can be verified on the test stand. Designing and manufacturing such stand is a demanding engineering task imposing other limitations.

3. Discretization of the problem

For the sake of the control design we shall now discretize system (1), so that it will be represented by a set of ordinary differential equations. For the sake of the control design we distinguish the terms associated with the control variable u, which is assumed to be equal to the sum of the squares of the inductions $u = B_1^2 + B_2^2$. The set of admissible controls will be denoted by $[0, u_{\max}]$, where the maximum admissible control $u_{\max} = 0.1\,T^2$, which follows from the assumed maximum inductions.

Consider an approximate solution to the partial equation of the pipe's motion in the form of a linear combination of cantilever beam eigenfunctions

$$w(\xi, t) = \sum_{j=1}^{n} W_j(\xi) Y_j(t), \tag{3}$$

$$W_j(\xi) = C_j \left[\cosh \frac{\lambda_j}{L}\xi - \cos \frac{\lambda_j}{L}\xi + \frac{\sin \lambda_j - \sinh \lambda_j}{\cos \lambda_j + \cosh \lambda_j} \left(\sinh \frac{\lambda_j}{L}\xi - \sin \frac{\lambda_j}{L}\xi \right) \right], \tag{4}$$

where the λ_j are consecutive roots of the characteristic equation $\cos\lambda \cosh\lambda = -1$, and the C_j are constants which normalize the shapes of the modes with respect to the norm induced by the scalar product $\int_0^L W_i W_j$. Applying Galerkin's procedure, one

obtains a set of n second-order ordinary differential equations for the vector of unknown generalized coordinates $\mathbf{Y} = \left(Y_i\right)_{n\times 1}$

$$\mathbf{M}\ddot{\mathbf{Y}} + \left(\mathbf{D} + v\mathbf{D}_{\mathbf{Cor}} + u\mathbf{D}_{\mathbf{act}}\right)\dot{\mathbf{Y}} + \left(\mathbf{S} + v^2\mathbf{S}_{\mathbf{in}}\right)\mathbf{Y} = \mathbf{0}, \tag{5}$$

where $\mathbf{M} = \left((m + m_f)\delta_{ij} + M_a W_i(\xi_a)W_j(\xi_a)\right)_{n\times n}$ is the mass matrix, $\mathbf{D} = \left(\left(E^* I(\lambda_j/L)^4\delta_{ij}\right)_{n\times n}\right.$ is the structural damping matrix, $\mathbf{D}_{\mathbf{Cor}} = \left(2m_f d_{ij}\right)_{n\times n}$ is the matrix that characterizes the damping generated by the Coriolis force, $\mathbf{D}_{\mathbf{act}} = \left(CW_i(\xi_a)W_j(\xi_a)\right)_{n\times n}$ is a matrix describing the influence of the actuators, $\mathbf{S} = \left(EI(\lambda_j/L)^4\delta_{ij} + \left(m + m_f\right)gb_{ij} + M_a g c_{ij} - \left(m + m_f\right)gd_{ij} - M_a g W_i(\xi_a)W_j'(\xi_a)\right)_{n\times n}$ is the structural stiffness matrix, $\mathbf{S}_{\mathbf{in}} = \left(m_f a_{ij}\right)$ is a matrix characterizing the inertia of the moving fluid, i.e., the effect that generates the flutter vibrations, $a_{ij} = \int_0^L W_i W_j''$, $b_{ij} = \int_0^L (L-\xi)W_i W_j''$, $c_{ij} = \int_0^L \mathbf{1}_{[0,\xi_a]} W_i W_j''$, $d_{ij} = \int_0^L W_i W_j'$, and δ_{ij} is Kronecker's delta.

Now reduce the order of the problem by the substitution $x_i = Y_i$, $x_{n+i} = \dot{Y}_i$, $i = 1, 2, \ldots, n$, gather the variables into the vector $\mathbf{x} = \left(x_i\right)_{2n\times 1}$. The dynamics of the control system is governed by the first-order bilinear differential equation

$$\dot{\mathbf{x}}(t) = \mathbf{A}\,\mathbf{x}(t) + u(t)\,\mathbf{B}\,\mathbf{x}(t), \quad \mathbf{x}(0) = \mathbf{x}^0, \tag{6}$$

where the following matrices allow separating the effects of the moving fluid and of the electromagnetic forces:

$$\mathbf{A} = \begin{pmatrix} \mathbf{0} & \mathbf{I} \\ -\mathbf{M}^{-1}\left(\mathbf{S} - v^2\,\mathbf{S}_{\mathbf{in}}\right) & -\mathbf{M}^{-1}\left(\mathbf{D} - v\,\mathbf{D}_{\mathbf{Cor}}\right) \end{pmatrix}, \tag{7}$$

$$\mathbf{B} = \begin{pmatrix} \mathbf{0} & \mathbf{0} \\ \mathbf{0} & -\mathbf{M}^{-1}\mathbf{D}_{\mathbf{act}} \end{pmatrix}. \tag{8}$$

The initial condition $\mathbf{x}^0$ is selected in the form of a deflection of the first cantilever's mode, more specifically,

$$x_1^0 \neq 0, \quad x_2^0 = \ldots = x_{2n}^0 = 0. \tag{9}$$

We have found, by examination, that $n = 10$ base functions are sufficient to describe the dynamics of the considered structure while keeping the size of the system eligible for efficient optimization. The criterion was the distance in the $\mathbb{L}^2$ norm between the (normalized) consecutive solutions over some period of time, i.e. on $[0, L] \times [0, T]$. This distance decreases with the growing number of base functions. Moreover, the number of 10 base functions turned out to be sufficient when analyzing similar, yet more complex, system of a pipe conveying fluid and the Beck column with electromagnetic devices of the transformer type [23,34]

4. Dynamical properties

4.1. The transition to flutter and the influence of the actuators

Assume for the time being that electromagnetic actuators are absent. The initial condition is in the form of the first eigenfunction of the cantilever beam, with the tip deflected by 5 mm and zero initial velocity. Fig. 2 illustrates the phenomena that occur when one increases the flow velocity. If $v = 0$, the system behaves like a simple vertical cantilever beam (Fig. 2(a)). For $v > 0$, two opposite effects take place: the Coriolis force that impedes the motion and the centrifugal force destabilizing the system. Since the former is linearly dependent on the flow velocity, it is more pronounced for its lower values (b). For higher values of the flow velocity, the inertial force, proportional to v^2, begins to dominate, which results in a greater frequency of the oscillations and weaker vibration suppression (c). When v reaches a critical value, which in this case amounts to 227.27 m s^{-1} (with two decimal points of precision), the system oscillates at a constant amplitude (d). Increasing the flow velocity beyond v^{cr} brings about an instability of the straight equilibrium position and exponentially growing vibrations (e).

Note that the effect of Coriolis damping was exploited by Sugiyama et al., who actively controlled the flow velocity to obtain efficient damping of the pipe, which in such a case could be used as a damper for elastic cantilever slender structures [35].

In subsequent sections we are going to study the performance of the proposed control method in all of the regimes except for the case $v = 0$, as it is the effect of the flow that we would like to focus on.

We now move on to the dynamics of the system with electromagnetic actuators. The influence of their position on the pipe ξ_a/L and control value $u = B_1^2 + B_2^2$ on the critical flow velocity is depicted in Fig. 3. The horizontal dashed line indicates a reference level without the actuators, i.e., for $u = 0$, which is $v_0^{\mathrm{cr}} = 227.27$ m s^{-1}. The solid line for $u = 0$ demonstrates that the effect of an added mass of the actuators may be both stabilizing as well as destabilizing, which was already a well-know result [6]. The viscous drag of the actuators with the applied voltage emphasizes this effect, see the curves for $u > 0$. What is interesting is that even low values of induction may significantly improve the stability of the system. For instance, assuming $B_1 = B_2 \approx 0.22$ T, we obtain $v_{0.1}^{\mathrm{cr}} = 348.55$ m s^{-1}, which is over 50% greater than the reference level and nearly 30% greater than v_0^{cr}. In fact, for low flow velocities it has turned out that the combined effect of the electromagnetic and Coriolis forces may result in overcritical damping.

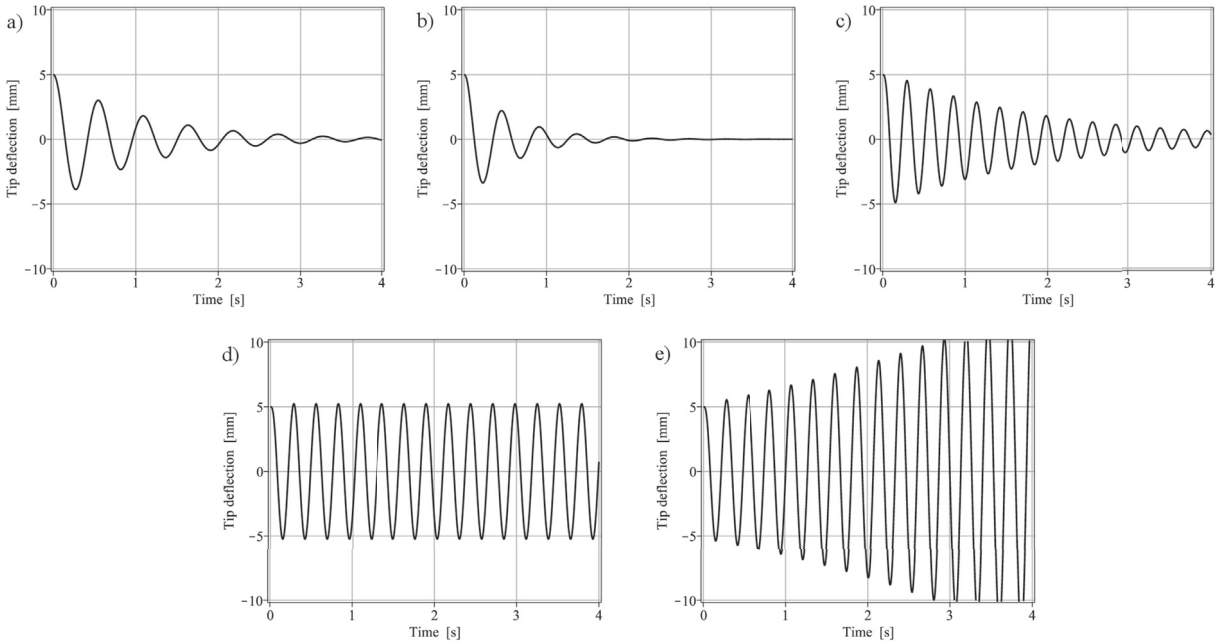

Fig. 2. Arising of the flutter vibrations: a) $v = 0$, b) $v = 120\,\mathrm{m\,s^{-1}}$, c) $v = 220\,\mathrm{m\,s^{-1}}$, d) $v = v^{\mathrm{cr}} = 227.27\,\mathrm{m\,s^{-1}}$, e) $v = 230\,\mathrm{m\,s^{-1}}$.

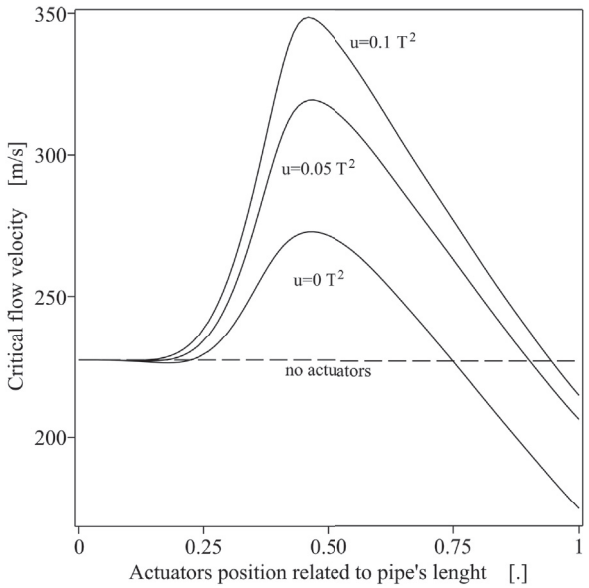

Fig. 3. Critical flow velocity v^{cr} as a function of the actuators' position x_a/L for selected values of the control input.

The control method is going to be evaluated for systems with three distinctively different positions of the actuators. First, we consider the actuators attached at $\xi_a = 0.10\,\mathrm{L}$, because the position close to the support may be justified from the technical point of view (for example most of the pipe may be immersed in a fluid). Next, we analyze $\xi_a = 0.46\,\mathrm{L}$, where the performance of the passive action is the highest. Finally, we investigate location $\xi_a = 1.00\,\mathrm{L}$, where the passive method is ineffective, but the analysis is motivated by curiosity.

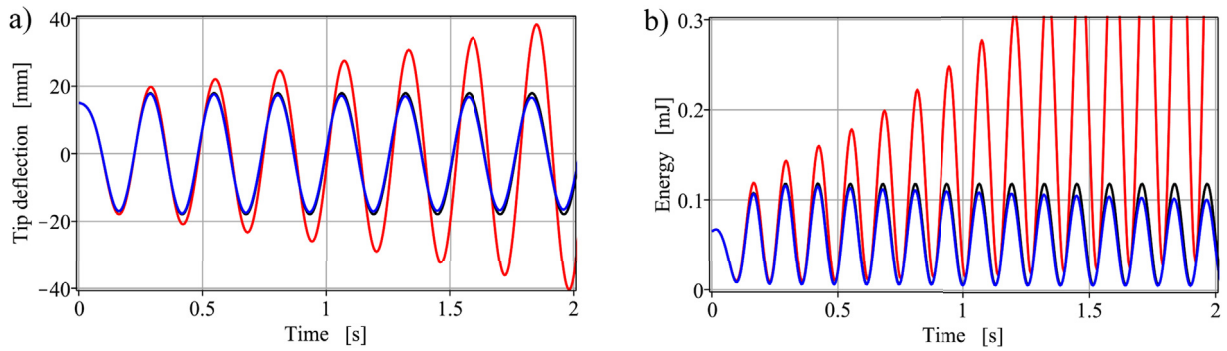

Fig. 4. Tip deflection (a) and potential energy (b) of the pipe with $u = 0.09\,\mathrm{T}^2$ (red, increasing oscillations), $u = 0.1\,\mathrm{T}^2$ (black) and $u = 0.101\,\mathrm{T}^2$ (blue, decreasing oscillations); $x_a = 0.46\,\mathrm{L}$ and $v = 348.55\,\mathrm{m\,s^{-1}} = v_{0.1}^{\mathrm{cr}}$. (For interpretation of the references to colour in this figure legend, the reader is referred to the Web version of this article.)

4.2. The energy of the pipe

Write $\mathbf{W}(\xi) = \left[W_1(\xi), \ldots, W_n(\xi)\right]^{\mathrm{T}}$, $\mathbf{x_I} = \left[x_1, \ldots, x_n\right]^{\mathrm{T}}$ and $\mathbf{x_{II}} = \left[x_{n+1}, \ldots, x_{2n}\right]^{\mathrm{T}}$. The following formula defines the elastic (strain) energy of the pipe:

$$v_{\mathrm{e}}^{\mathrm{pipe}}(t) = \int_0^L \frac{1}{2} EI \left(\frac{\partial^2 w}{\partial \xi^2}(\xi, t) \right)^2 \mathrm{d}\xi = \frac{1}{2} EI \mathbf{x}_{\mathbf{I}}^{\mathrm{T}}(t) \int_0^L \mathbf{W}''(\xi) \mathbf{W}''(\xi)^{\mathrm{T}} \mathrm{d}\xi \mathbf{x}_{\mathbf{I}}(t) = \frac{1}{2} \mathbf{x}^{\mathrm{T}}(t) \mathbf{Q} \mathbf{x}(t). \tag{10}$$

Here, the energy matrix

$$\mathbf{Q} = \begin{bmatrix} EI \int_0^L \mathbf{W}'' \mathbf{W}''^{\mathrm{T}} & \mathbf{0} \\ \mathbf{0} & \mathbf{0} \end{bmatrix} \tag{11}$$

is symmetric and positive semidefinite.

Fig. 4 demonstrates the tip deflection $w(L, t)$ and the potential energy of the pipe $v_{\mathrm{e}}^{\mathrm{pipe}}(t)$ for the control inputs $u = 0.09, 0.1$ and $0.101\,\mathrm{T}^2$ and flow velocity $v = v_{0.1}^{\mathrm{cr}} = 348.55\ \mathrm{m\ s^{-1}}$. For the conservative case, $u = u_{\max} = 0.1\,\mathrm{T}^2$, the oscillations of the energy remain at the same level. For $u = 0.09\,\mathrm{T}^2$ we observe an unstable case with an increase of the energy's oscillations. In order to obtain a stable case with a decrease of the energy's amplitudes, we need to exceed the admissible control value $u = 0.101\,\mathrm{T}^2$.

A complete description of the mechanical energy of the system is complicated, since it involves not only the kinetic energy of the pipe and additional mass, but also components related to the flow (our system is a part of the space limited by the pipe, not just the pipe), see for example [4]. Nevertheless, it has turned out that a control design based solely on the pipe's potential energy works fine. The potential energy can be fairly used to justify both the system's stability and the performance of the optimal controller. This is because the system exhibits periodic pattern of vibrations in the entire range of considered flow velocities. Thus the average value of the potential energy of the pipe over a period of time $[0, T]$ reflects how strongly the pipe is suppressed, providing that T is greater than the period of oscillations. Obviously we do not know if the control changes the energy of the moving fluid.

5. Stabilizability

Let $Ep(u(t))$ stand for the pipe's elastic energy (10) computed for the control function $u(t)$ and integrated over the time interval $[0, T], T > 0$:

$$Ep(u(t)) = \frac{1}{2} \int_0^T \mathbf{x}^T(t)\, \mathbf{Q}\, \mathbf{x}(t)\, \mathrm{d}t. \tag{12}$$

In the previous section, it was demonstrated that for the maximum admissible control $u_{\max}$ and the corresponding critical flow $v_{u_{\max}}^{cr}$, the system exhibits a conservative behavior with the total energy $Ep(u_{\max})$. It was also seen that for a fixed control input $u \in [0, u_{\max})$, the system exhibits an instability that can be identified as an increase of the energy $Ep(u) > Ep(u_{\max})$. Now we are interested in whether there exists a control function $u(t) \in [0, u_{\max}]$ describing a variable magnetic field that results in a reduction of the system's energy compared to the conservative case $Ep(u(t)) < Ep(u_{\max})$. The existence of such a control can be considered as the ability of the controller to dissipate some portion of the energy $Ep(u_{\max})$, and thus to stabilize the system's

vibration.

For system (6), we introduce the adjoint state dynamics represented by

$$\dot{\mathbf{p}}(t) = -\mathbf{A}^T\mathbf{p}(t) - u(t)\,\mathbf{B}^T\mathbf{p}(t) + \mathbf{Q}\,\mathbf{x}(t), \quad \mathbf{p}(T) = 0\,. \tag{13}$$

The following proposition gives a sufficient condition for the existence of a control providing $Ep(u(t)) < Ep(u_{\max})$.

Proposition 1. *Let $\mathbf{x}_{u_{\max}}(t)$ and $\mathbf{p}_{u_{\max}}(t)$ be the solutions to the state (6) and the adjoint state (13) equations when $v = v^{cr}_{u_{\max}}$ and the following constant control function is applied: $u(t) = u_{\max}, \forall t \in [0, T]$. If there exists an interval $[t_1, t_2] \subseteq [0, T]$ such that for all $t \in [t_1, t_2]$ we have $\mathbf{p}^T_{u_{\max}}(t)\,\mathbf{B}\,\mathbf{x}_{u_{\max}}(t) < 0$, then there also exists a control $u^*(t) \in [0, u_{\max}]$ such that $Ep(u^*(t)) < Ep(u_{\max})$.*

Proof. Assuming $u^*(t) = u_{\max} + \delta u$, where δu stands for an infinitesimal change of the control, the differential of the system's energy can be represented by

$$Ep(u_{\max} + \delta u) - Ep(u_{\max}) = \delta Ep(u_{\max})(\delta u) + r_{Ep}(u_{\max}, \delta u)\,. \tag{14}$$

Here $\delta Ep(u_{\max})(\delta u)$ is the first variation of $Ep(u_{\max})$ and $r_{Ep}(u_{\max}, \delta u)/\|\delta u\| \to 0$ as $\|\delta u\| \to 0$. For a sufficiently small δu the sign of the right hand side of (14) is determined by the sign of the variation. Thus, we need to demonstrate that the condition $\mathbf{p}^T_{u_{\max}}(t)\,\mathbf{B}\,\mathbf{x}_{u_{\max}}(t) < 0$ implies $\delta Ep(u_{\max})(\delta u) < 0$ where $\delta u : (u_{\max} + \delta u) \in [0, u_{\max}]$.

Using the state dynamics equation (6) we can rewrite (12):

$$Ep(u) = \int_0^T \left(\frac{1}{2}\mathbf{x}^T\,\mathbf{Q}\,\mathbf{x} + \mathbf{p}^T(\dot{\mathbf{x}} - \mathbf{A}\,\mathbf{x} - u\,\mathbf{B}\,\mathbf{x})\right) \mathrm{d}t\,. \tag{15}$$

By introducing the Hamiltonian

$$H(\mathbf{x}, \mathbf{p}, u) = \mathbf{p}^T\,(\mathbf{A}\,\mathbf{x} + u\,\mathbf{B}\,\mathbf{x}) - \frac{1}{2}\mathbf{x}^T\,\mathbf{Q}\,\mathbf{x}, \tag{16}$$

the energy (15) can be represented by

$$Ep(u) = \int_0^T \left(\mathbf{p}^T\,\dot{\mathbf{x}} - H(\mathbf{x}, \mathbf{p}, u)\right) \mathrm{d}t\,. \tag{17}$$

An infinitesimal change δu causes variations of the functions $\delta\mathbf{x}$, $\delta\dot{\mathbf{x}}$, $\delta\mathbf{p}$ which result in the following variation of the system's energy:

$$\delta Ep\,(u)\,(\delta u) = \int_0^T \left(-\frac{\partial H}{\partial u}\,\delta u - \left(\frac{\partial H}{\partial \mathbf{x}}\right)^T \delta\mathbf{x}\right) \mathrm{d}t \quad + \int_0^T \left(\mathbf{p}^T\delta\dot{\mathbf{x}} + \left(\dot{\mathbf{x}} - \frac{\partial H}{\partial \mathbf{p}}\right)^T \delta\mathbf{p}\right) \mathrm{d}t. \tag{18}$$

The last term in (18) vanishes, since we have

$$\dot{\mathbf{x}} = \frac{\partial H}{\partial \mathbf{p}}\,. \tag{19}$$

Under the assumption

$$\delta\dot{\mathbf{x}} = \frac{d}{dt}\,(\delta\mathbf{x}) \tag{20}$$

an integration by parts yields

$$\delta Ep\,(u)\,(\delta u) = -\int_0^T \frac{\partial H}{\partial u}\,\delta u\,\mathrm{d}t \; - \int_0^T \left(\dot{\mathbf{p}} + \frac{\partial H}{\partial \mathbf{x}}\right)^T \delta\mathbf{x}\,\mathrm{d}t + \left[\mathbf{p}^T\delta\mathbf{x}\right]_0^T\,. \tag{21}$$

From (13) we observe that

$$\dot{\mathbf{p}} + \frac{\partial H}{\partial \mathbf{x}} = 0, \quad \mathbf{p}(T) = 0\,. \tag{22}$$

Moreover, the initial condition in (6) implies $\delta\mathbf{x}(0) = 0$. Therefore, the two last terms in (21) vanish, and eventually we obtain

$$\delta Ep(u)(\delta u) = -\int_0^T \frac{\partial H}{\partial u}\,\delta u\,\mathrm{d}t = -\int_0^T \mathbf{p}^T\,\mathbf{B}\,\mathbf{x}\,\delta u\,\mathrm{d}t\,. \tag{23}$$

Now, let the variation of the control be given by

$$\delta u = \begin{cases} 0, & t \in [0, t_1) \\ \epsilon < 0, & t \in [t_1, t_2] \\ 0, & t \in (t_2, T]\,. \end{cases} \tag{24}$$

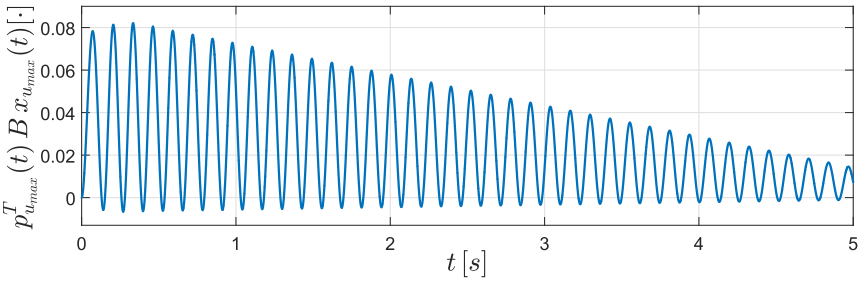

Fig. 5. Evolution of the trajectory of the function $\mathbf{p}^T_{u_{\max}}(t)\,\mathbf{B}\,\mathbf{x}_{u_{\max}}(t)$. The negative values of the function imply the existence of a stabilizing control $u^*(t)$.

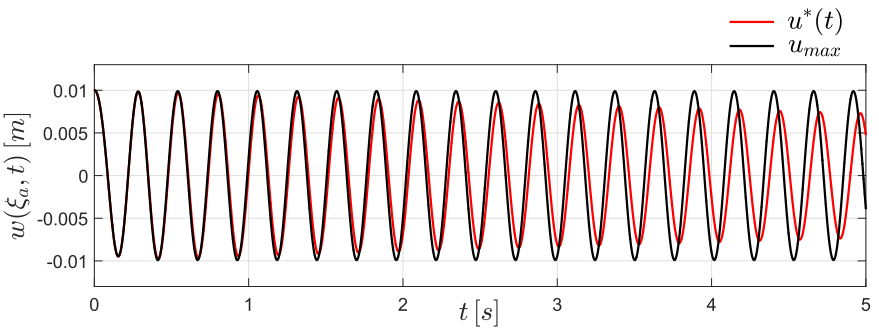

Fig. 6. Comparison of pipe's deflection $w(\xi_a, t)$ when fixed conservative control $u_{\max}$ and variable stabilizing control $u^*(t)$ are applied.

For a sufficiently small ϵ we have $(u_{\max} + \delta u) \in [0, u_{\max}]$. From (23) and (24) we conclude that the condition $\mathbf{p}^T_{u_{\max}}(t)\,\mathbf{B}\,\mathbf{x}_{u_{\max}}(t) < 0$ for all $t \in [t_1, t_2]$ implies

$$\delta Ep(u_{\max})(\delta u) = -\int_{t_1}^{t_2} \mathbf{p}^T_{u_{\max}}\,\mathbf{B}\,\mathbf{x}_{u_{\max}}\,\epsilon\,\mathrm{d}t < 0, \tag{25}$$

which completes the proof.

In order to illustrate the result of Proposition 1, we shall now investigate the system considering the following parameters: $\xi_a = 0.46\,\mathrm{L}$, $v = 348.55\,\mathrm{m\,s^{-1}}$, $u_{\max} = 0.1\,\mathrm{T}^2$. For the initial condition we take $w(\xi, 0) = 10^{-2} W_1(\xi)/W_1(\xi_a)$ m. Recall from Section 4.1 that the assumed flow velocity is equal to the critical value for the maximum admissible magnetic field $v = v^{cr}_{u_{\max}}$. Therefore, for every fixed magnetic field $u \in [0, u_{\max}]$, the system is either conservative or unstable. We shall justify the existence of a stabilizing control $u^*(t) \in [0, u_{\max}]$ by simulating the trajectories $\mathbf{x}_{u_{\max}}(t)$ and $\mathbf{p}_{u_{\max}}(t)$ for $t \in [0, T]$, where we select $T = 5\,\mathrm{s}$. In the selection of the time T, one should first identify the periodicity of the state/adjoint state dynamics. It is advisable that T should be taken to be no less than the period of the state/adjoint state, so as to allow $\mathbf{p}^T_{u_{\max}}\,\mathbf{B}\,\mathbf{x}_{u_{\max}}$ to change its sign to negative.

The trajectory of $\mathbf{p}^T_{u_{\max}}\,\mathbf{B}\,\mathbf{x}_{u_{\max}}$ is depicted in Fig. 5. One can immediately detect the time periods where the condition $\mathbf{p}^T_{u_{\max}}\,\mathbf{B}\,\mathbf{x}_{u_{\max}} < 0$ is fulfilled. An example of a stabilizing control $u^*(t)$ is demonstrated in Fig. 7. Observe that the control variable is switched twice per cycle, namely, in the time instants of the extreme deflections of the pipe, when its velocity is close to zero. In Fig. 6, we compare the deflection $w(\xi_a, t)$ generated by the control function $u^*(t)$ with that generated by the fixed control $u_{\max}$. By applying the control $u^*(t)$, the total energy Ep is reduced by 24%.

6. Optimal control

In the previous section, we considered the feasibility of designing a function $u(t)$ that results in a lower value of the measure Ep of the pipe's elastic energy than any constant control $u \in [0, u_{\max}]$. In particular, we demonstrated that $u(t)$ can be a stabilizing control if $u = u_{\max}$ results in the conservative case, i.e., for $v = v^{cr}_{u_{\max}}$. In practical control design, one should take into account not only the stabilizing performance but also the possibility of reducing the energy consumed by the actuators. The instantaneous power consumed by the electromagnets operating with the inductions $B_1(t), B_2(t)$ can be represented by $B_1^2(t) + B_2^2(t) = u(t)$. Therefore, for the total electric energy consumed by the actuators, we shall use

$$Ee(u(t)) = \frac{1}{2}\int_0^T u(t)\,\mathrm{d}t\,. \tag{26}$$

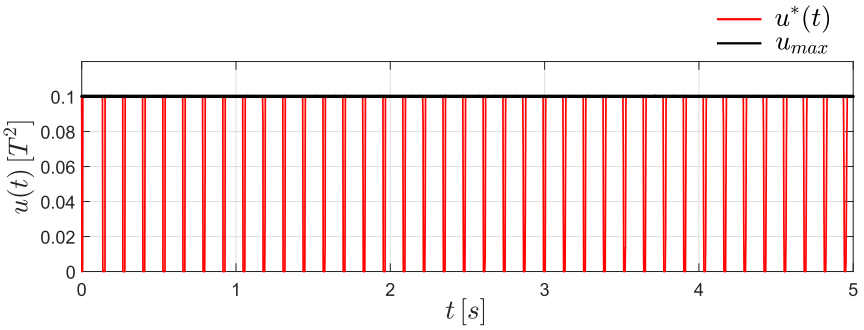

Fig. 7. Fixed conservative control $u_{\max}$ and variable stabilizing control $u^*(t)$.

The remainder of this paper is devoted to the design and quantitative analysis of controls providing optimal performance, as measured by *Ep* and *Ee*.

6.1. The optimal control problem

We consider the following optimal control problem.

$$\begin{aligned} &\text{Find} \quad u_{opt}(u(t)) = \operatorname{argmin} J(u(t)) = \frac{1}{2}\int_0^T \left(\mathbf{x}^T(t)\,\mathbf{Q}\,\mathbf{x}(t) + \alpha\, u^2(t)\right) \mathrm{d}t \\ &\text{Subject to} \quad \dot{\mathbf{x}}(t) = \mathbf{A}\,\mathbf{x}(t) + u(t)\,\mathbf{B}\,\mathbf{x}(t), \quad \mathbf{x}(0) = \mathbf{x}_0, \\ &\qquad\qquad u(t) \in \left[0, u_{\max}\right]. \end{aligned} \tag{27}$$

For the objective J to be minimized, we select the pipe's elastic energy *Ep* weighted by the square of the electric energy Ee^2 (for the weighting factor, we assume $\alpha > 0$). In this selection, we opt for the quadratic term $\alpha u^2(t)$, aiming at ensuring the convexity of the functional J with respect to the decision parameter $u(t)$. This will allow us to solve the problem efficiently by using a gradient-based method.

Due to the middle term in the right hand side of the state equation (6), the system is classified as bilinear [36]. The existence of a solution to the bilinear optimal control problem (27) follows from Filippov's theorem and the continuity of the objective functional (for details, see Ref. [37]).

6.2. The method of solution

In order to solve problem (27), we shall develop an iterative algorithm based on the method of steepest descent. First, we need to estimate the relevant derivatives corresponding to the directions of the descent of the objective functional for the decision parameter. By introducing the Hamiltonian

$$H(\mathbf{x}, \mathbf{p}, u) = \mathbf{p}^T(\mathbf{A}\,\mathbf{x} + u\,\mathbf{B}\,\mathbf{x}) - \frac{1}{2}\mathbf{x}^T\mathbf{Q}\,\mathbf{x} - \frac{1}{2}\alpha\, u^2 \tag{28}$$

and the adjoint state dynamics

$$\dot{\mathbf{p}}(t) = -\frac{\partial H}{\partial \mathbf{x}} = -\mathbf{A}^T\mathbf{p}(t) - u(t)\,\mathbf{B}^T\mathbf{p}(t) + \mathbf{Q}\,\mathbf{x}(t), \quad \mathbf{p}(T) = 0\,. \tag{29}$$

the objective functional can be represented by

$$J(u) = \int_0^T \left(\mathbf{p}^T\dot{\mathbf{x}} - H(\mathbf{x}, \mathbf{p}, u)\right) \mathrm{d}t\,. \tag{30}$$

Performing the analogous steps to (18)–(23), we conclude that the derivative of the objective functional J with respect to the control function u is

$$\frac{\delta J}{\delta u} = -\int_0^T \frac{\partial H}{\partial u}\,\mathrm{d}t = -\int_0^T \left(\mathbf{p}^T\mathbf{B}\,\mathbf{x} - \alpha\, u\right) \mathrm{d}t\,. \tag{31}$$

Now we can extract from (31) the derivative of J with respect to the control value at a specific time instant $t \in [0, T]$:

$$\left(\frac{\delta J}{\delta u}\right)_{|t} = -\int_0^T \left(\mathbf{p}^T(t')\,\mathbf{B}\,\mathbf{x}(t') - \alpha\, u(t')\right) \delta(t' - t)\,\mathrm{d}t'\,. \tag{32}$$

Here, $\delta(\cdot)$ stands for the Dirac delta function. Using the sifting property of the Dirac delta function we conclude that

$$\left(\frac{\delta J}{\delta u}\right)_{|t} = -\mathbf{p}^T(t)\,\mathbf{B}\,\mathbf{x}(t) + \alpha\, u(t)\,. \tag{33}$$

Having at our disposal the formulas for the derivative of the objective functional, we are ready to build an iterative algorithm for finding the optimal control function $u_{opt}(t)$. In order to fulfill the constraints defined by the admissible control set $[0, u_{\max}]$, we introduce the projection

$$\mathrm{Proj}\,(u\,(t)) = \begin{cases} 0, & u\,(t) < 0 \\ u\,(t)\,, & 0 \le u\,(t) \le u_{\max} \\ u_{\max}, & u\,(t) > u_{\max}\,. \end{cases} \tag{34}$$

For the time instant t the value of the control function will be updated by using the following sequence:

$$u^{l+1}(t) = \mathrm{Proj}\left(u^l(t) - \gamma\left(\frac{\delta J}{\delta u}\right)_{|t}\right), \quad \gamma > 0, \quad l = 0, 1, \ldots, l_{\max}\,. \tag{35}$$

For the initial iteration, $l = 0$, we will assume the control $u^l_{opt}(t) = u_{\max}$ for all $t \in [0, T]$. In the iterative algorithm, we will introduce the maximal admissible number of iterations, denoted by $l_{\max}$. Its value is selected to guarantee that the control update is terminated in the required time. The parameter $\gamma > 0$ is assumed to be suitably small, and is supposed to be determined based on trial runs. In order to guarantee a monotonic decrease of the value of the objective functional $J(u^l(t))$ at each iteration l, we will perform a backtracking line-search by modifying the step size γ by $\gamma = \kappa \cdot \gamma$, $\kappa \in (0, 1)$. The optimization algorithm is composed of the following steps:

Step 1.	Set $l = 0$ and the initial control $u^l(t) = u_{\max}$ for all $t \in [0, T]$. Assume γ and ϵ are small positive numbers. Assume the maximal number of iterations $l_{\max}$. Select $\kappa \in (0, 1)$.
Step 2.	Solve the state equation (6) by substituting $u(t) = u^l(t)$.
Step 3.	By backward integration solve the adjoint state equation (29) by substituting the solution into the state equation (Step 2) and $u(t) = u^l(t)$.
Step 4.	Evaluate the derivative (33) by substituting the solution into the state equation (Step 2), the solution to the adjoint state equation (Step 3) and $u(t) = u^l(t)$.
Step 5.	Update the control $u^{l+1}(t)$ using (35).
Step 6.	Compute the value of the objective function $J(u(t))$ for $u^{l+1}(t)$. If $J(u^{l+1}(t)) < J(u^l(t))$, then set $l = l + 1$ and go to Step 7. Otherwise, modify the step-size γ by $\gamma = \kappa \cdot \gamma$, and go to Step 4.
Step 7.	Check if any of the terminal conditions is fulfilled: $\mid J(u^l(t)) - J(u^{l-1}(t)) \mid / J(u^{l-1}(t) < \epsilon$ or $l = l_{\max}$. If not, then go to Step 2.Otherwise, set $u_{opt}(t) = u^l(t)$ and STOP.

For the convenience of the reader the schematic representation of the algorithm is presented in Appendix in Fig. 16.

7. Numerical study

In this section, relying on the proposed algorithm, we will examine the performance of the optimal control of (6). The simulations were carried out for nine scenarios, where we assume the following positions of the actuators: $\xi_a = 0.10\,\mathrm{L}, 0.46\,\mathrm{L}, 1.00\,\mathrm{L}$. For each position, we consider the flow velocities $v = 0.50\,v^{cr}_{0.1}, 0.99\,v^{cr}_{0.1}, 1.01\,v^{cr}_{0.1}$. Here, for $\xi_a = 0.10\,\mathrm{L}$, $\xi_a = 0.46\,\mathrm{L}$, and $\xi_a = 1.00\,\mathrm{L}$, we have the critical flow velocity $v^{cr}_{0.1}$ equal to 227.17, 348.55 and 215.13 m s^{-1}, respectively. For the initial condition, we take $w(\xi, 0) = 10^{-2}W_1(\xi)/W_1(\xi_a)$ m for $\xi_a = 0.50\,\mathrm{L}$, $\xi_a = 1.00\,\mathrm{L}$, and $w(\xi, 0) = 10^{-3}W_1(\xi)/W_1(\xi_a)$ m for $\xi_a = 0.10\,\mathrm{L}$.

In each scenario, we will compare the dynamics generated by the optimal solution $u_{opt}(t)$ with that generated by the passive control u_{pass}, which we define as a constant control consuming the same amount of electric energy as the optimal solution: $Ee(u_{pass}) = Ee(u_{opt}(t))$. From (26) we obtain

$$u_{pass} = \frac{1}{T}\int_0^T u_{opt}(t)\,\mathrm{d}t\,. \tag{36}$$

For the simulation horizon, we assume $T = 2$ s. The time interval $[0, T]$ is represented by $2 \cdot 10^5$ samples. This setting provides stable solutions to the state and the adjoint state equations acquired by using the Runge–Kutta 4th order scheme.

For the optimization algorithm, we assume the following parameters (see Step 1): $\gamma = 10^{-1}$, $\epsilon = 10^{-4}$, $l_{\max} = 10^3$, $\kappa = 0.75$. In the selection of the weighting parameter α (see 27), we prioritize the reduction of the elastic energy Ep. The parameter α is assumed constant over the whole optimization process, and is computed to fulfill the equality $Ep = 10^2 \cdot \alpha Ee^2$ at the initial iteration of the algorithm.

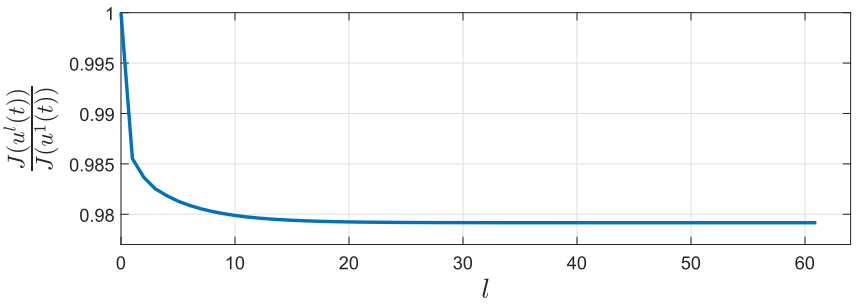

Fig. 8. Evolution of the objective functional during the iteration of the optimization procedure for the case $\xi_a = 0.46L$, $v = 0.50\, v^{cr}_{0.1}$. The procedure was terminated after $l = 61$ iterations by the condition $|J(u^l(t)) - J(u^{l-1}(t))|/J(u^{l-1}(t) < \epsilon$.

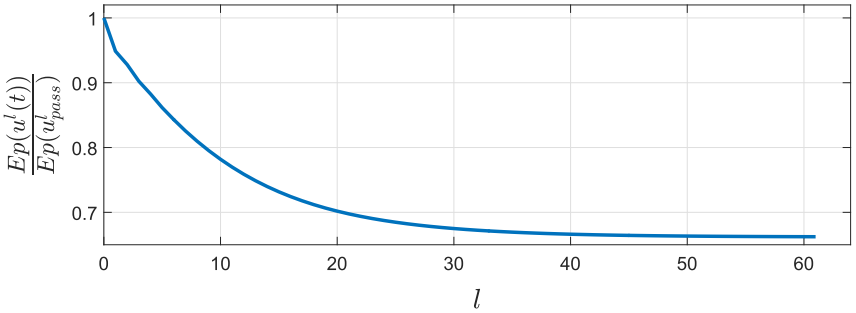

Fig. 9. Evolution of the relative energy of the elastic pipe during the iteration of the optimization algorithm for the case $\xi_a = 0.46L$, $v = 0.50\, v^{cr}_{0.1}$.

7.1. Cases for $\xi_a = 0.46\,L$

We begin with the case of $\xi_a = 0.46\,\mathrm{L}$ and the low subcritical flow velocity $v = 0.50\, v^{cr}_{0.1}$. In order to examine the convergence of the optimization algorithm, Fig. 8 presents the evolution of the objective functional J during the iteration process (the values of the objective functional are normalized to that computed for the initial iteration $l = 0$). Performing the steepest gradient procedure, we can observe a rapid, monotonic decrease of J. Similarly, we examine a monotonic decrease of the relative value of the pipe's elastic energy $Ep(u_{opt})/Ep(u_{pass})$, as shown in Fig. 9. The procedure was terminated at iteration $l = 61$ (after 215 s using a standard PC with Intel Xeon, 3.00 GHz), where the terminal condition $|J(u^l(t)) - J(u^{l-1}(t))|/J(u^{l-1}(t) < \epsilon$ was satisfied. As a result of the optimization, we obtain a 33.8% reduction of the elastic energy compared to the passive solution (for a detailed comparison of the elastic energies, see Table 2). The observed results of the convergence of the optimization algorithm remain intact for the rest of the considered scenarios.

Fig. 10 presents the optimal control and the corresponding passive control $u_{pass} = 0.0522\,\mathrm{T}^2$ in the case of $\xi_a = 0.46L$, $v = 0.50\, v^{cr}_{0.1}$. At the first stage of the simulation, one can see a periodic switching pattern of the optimal control's trajectory. Recall from Ref. [38] that the solution to a bilinear optimal control problem such as (27) is of the bang-bang structure if the objective functional does not explicitly depend on the control, e.g., in our case for $\alpha = 0$. Since we assume $\alpha > 0$, the optimal control function exhibits a tendency to decrease its value, providing a lower consumption of electric energy. In the considered case, a gradual decrease of the control value is observed for $t > 0.7$ s, where the amplitudes iof the pipe's vibration remain at a

Table 2
Comparison of the performance of the optimal control for the considered flow velocities and the positions of the electromagnets. For each case the value represents the pipe's potential energy normalized to the corresponding passive strategy, i.e., $Ep(u_{opt}(t))/Ep(u_{pass})$.

ξ_a	$0.50\, v^{cr}_{0.1}$	$0.99\, v^{cr}_{0.1}$	$1.01\, v^{cr}_{0.1}$
0.10 L	0.9985	0.9938	0.9876
0.46 L	0.6624	0.1511	0.0507
1.00 L	0.7730	0.6071	0.4047

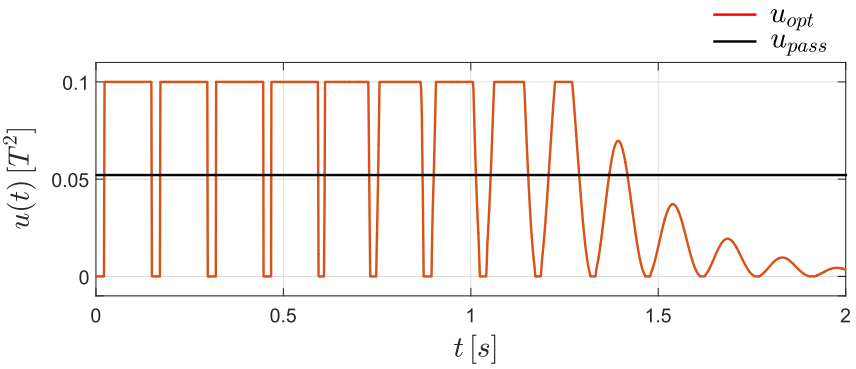

Fig. 10. The optimal control $u_{opt}(t)$ and the corresponding passive control $u_{pass} = 0.0522\,\mathrm{T}^2$ in the case of $\xi_a = 0.46L$, $v = 0.50\,v_{0.1}^{cr}$.

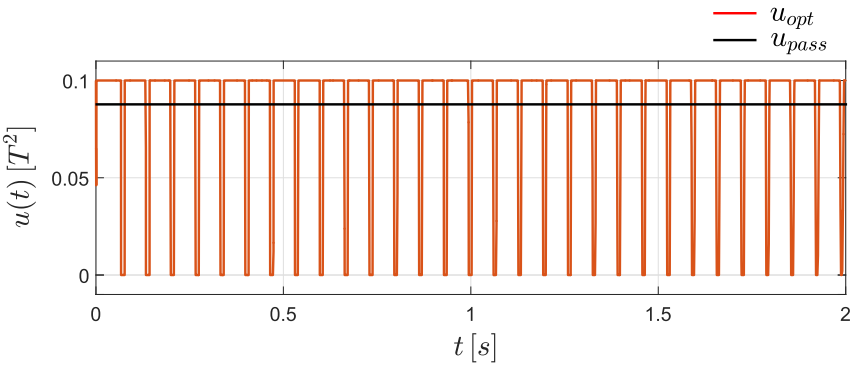

Fig. 11. The optimal control $u_{opt}(t)$ and the corresponding passive control $u_{pass} = 0.0870\,\mathrm{T}^2$ in the case of $\xi_a = 0.46L$, $v = 0.99\,v_{0.1}^{cr}$.

modest level (see Fig. 13). Further analysis on the trajectory $w(\xi_a, t)$ confirms the high performance of the optimal control in stabilizing the pipe's vibration. Compared to the passive control, the first two peak deflections at $t = 0.14\,\mathrm{s}$ and $t = 0.28\,\mathrm{s}$ are reduced by 31.7% and 52.2%, respectively. For $t > 1\,\mathrm{s}$, for the optimal trajectory, we observe negligible levels of vibration: $|w(\xi_a, t)| < 10^{-6}\,\mathrm{m}$.

Now we consider the case of the high subcritical flow $v = 0.99\,v_{0.1}^{cr}$. For comparison of the optimal control and the corresponding passive control $u_{pass} = 0.0870\,\mathrm{T}^2$ the reader is referred to Fig. 11. Unlike in the previous case, the periodic switching control pattern is preserved for the whole simulation. This results from the significantly higher deflections of the pipe (see Fig. 14) and the assumed weighting parameter, which prioritizes the reduction of the elastic energy over the decrease of the

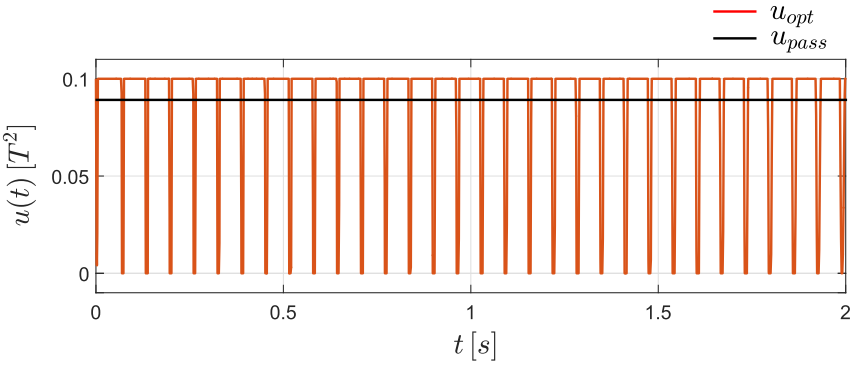

Fig. 12. The optimal control $u_{opt}(t)$ and the corresponding passive control $u_{pass} = 0.0894\,\mathrm{T}^2$ in the case of $\xi_a = 0.46L$, $v = 1.01\,v_{0.1}^{cr}$.

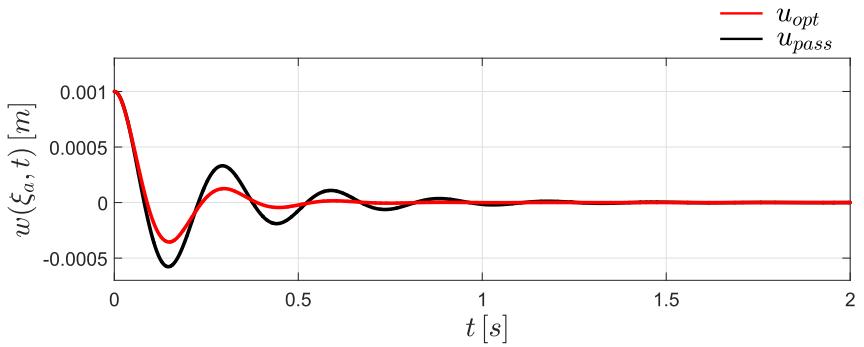

Fig. 13. Comparison of pipe's deflection $w(\xi_a, t)$ for the optimal and the passive control in the case of $\xi_a = 0.46L$, $v = 0.50\, v_{0,1}^{cr}$.

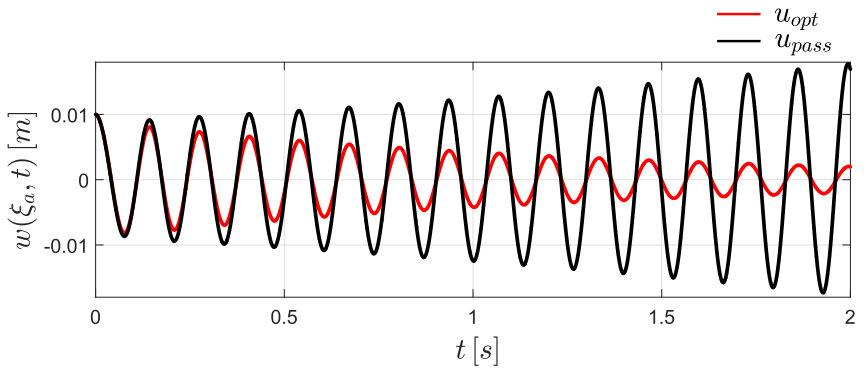

Fig. 14. Comparison of pipe's deflection $w(\xi_a, t)$ for the optimal and the passive control in the case of $\xi_a = 0.46L$, $v = 0.99\, v_{0,1}^{cr}$.

consumed electric energy. The optimal deflection trajectory is stable and its rate of decrease allows for a reduction of 81.2% of the peak amplitude for the assumed simulation time. In terms of the elastic energy metric, the optimal control outperforms the unstable passive one by 84.9%.

For the low supercritical flow $v = 1.01\, v_{0,1}^{cr}$, we examine the unstable optimal solution depicted in Fig. 15. Compared to the passive strategy $u_{pass} = 0.0894\,\mathrm{T}^2$, the optimal control notably reduces the state's rate of divergence. As a result, the ending peak amplitude of the deflection trajectory is cut by 85.4% and the elastic energy metric is decreased by 84.9%. From Fig. 12 one can see that, as in the previous case, the optimal control function relies on a periodically switching structure.

7.2. The cases $\xi_a = 0.10\,L$ and $\xi_a = 1.00\,L$

In this section, we briefly summarize the performance of the optimal control for the alternative locations of the electromagnetic actuator. All the qualitative observations on the optimal control structures and the resulting system dynamics presented

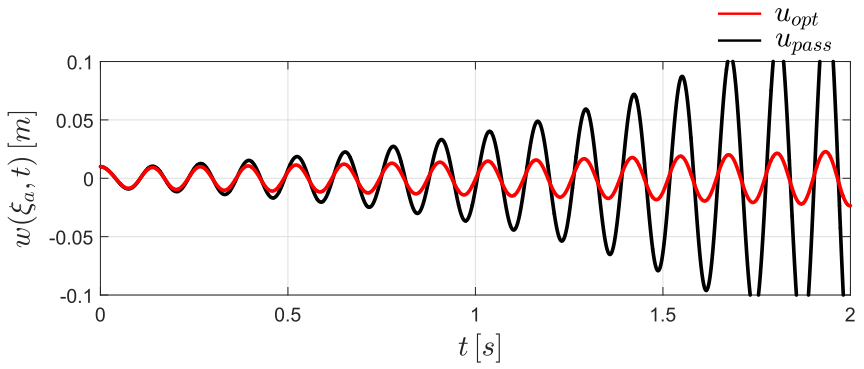

Fig. 15. Comparison of pipe's deflection $w(\xi_a, t)$ for the optimal and the passive control in the case of $\xi_a = 0.46L$, $v = 1.01\, v_{0,1}^{cr}$.

in the cases of $\xi_a = 0.46\,\mathrm{L}$ are also valid for $\xi_a = 0.10\,\mathrm{L}$ and $\xi_a = 1.00\,\mathrm{L}$. We limit our attention to the quantitative analysis.

Based on the analysis of the energy function (see Table 2) we immediately see a marginal influence of the control for all the cases of $\xi_a = 0.10\,\mathrm{L}$. The minor 0.2%–1.2% improvement of the optimal control when compared to the passive solution results from the low transverse velocities of the pipe at the point ξ_a, and thus the low damping forces generated by the electromagnets. The authors also validated the comparable optimal control performance when increasing/decreasing the weighting parameter α.

Eventually, we examined the cases with the actuator located at the end of the pipe $\xi_a = 1.00\,\mathrm{L}$. For the low subcritical flow $v = 0.50\,v_{0.1}^{cr}$, we observed a rapid convergence of the optimal deflection trajectory, resulting in a 22.7% reduction of the elastic energy metric. In the case of the high subcritical flow $v = 0.99\,v_{0.1}^{cr}$, the optimally controlled system exhibited a stable deflection trajectory with a lower rate of decrease than for $\xi_a = 0.46\,\mathrm{L}$. The associated energy was decreased by 39.3% compared to the unstable solution generated by the passive control. For the low supercritical flow $v = 1.01\,v_{0.1}^{cr}$, we observe a moderately unstable optimal deflection trajectory resulting in a 59.5% improvement of elastic energy compared to the highly unstable passive solution.

8. Conclusions

The combined effects of the additional mass and the viscous-type electromagnetic force generated by the devices of the motional type can remarkably affect dynamical properties of the cantilever pipe discharging fluid. The passive action of the actuators attached near the half of the length of the pipe increases the critical flow velocity by ~50% comparing to the pipe without the actuators. This improvement was obtained for moderate values of the magnetic flux densities in electromagnetic circuits, which can be easily obtained in practice (~0.22 T). The proposed method of stabilization is based on contact-less devices, thus its application may be especially advisable for slender structures, whose stability could be affected by the use of force actuators directly attached to the structure.

The actuators can be controlled by varying the supplied voltage, which enables the implementation of control strategies. First, we have proved the existence of a control strategy that is able to stabilize the system in a range of control values for which all passive methods cannot do this. Then we developed an algorithm to solve the optimal control problem of minimizing the average potential energy of the pipe combined with the electrical energy of the actuators. The performance of the method was assessed for the pipe systems with various actuators' positions and flow velocities. It turned out that the controlled strategy can stabilize the system better than the passive method, while consuming the same amount of electrical energy.

The periodic pattern of the optimal control for the system with near-critical values of the flow velocity allows its state-feedback parametrization and design of a practical and robust closed-loop control system. This design as well as an experimental validation of the method on the already built test-stand of a pipe conveying air are going to be the next steps of the research.

Acknowledgement

The research was supported by the National Science Centre, Poland under grant agreement UMO-2015/17/D/ST8/02434.

Appendix

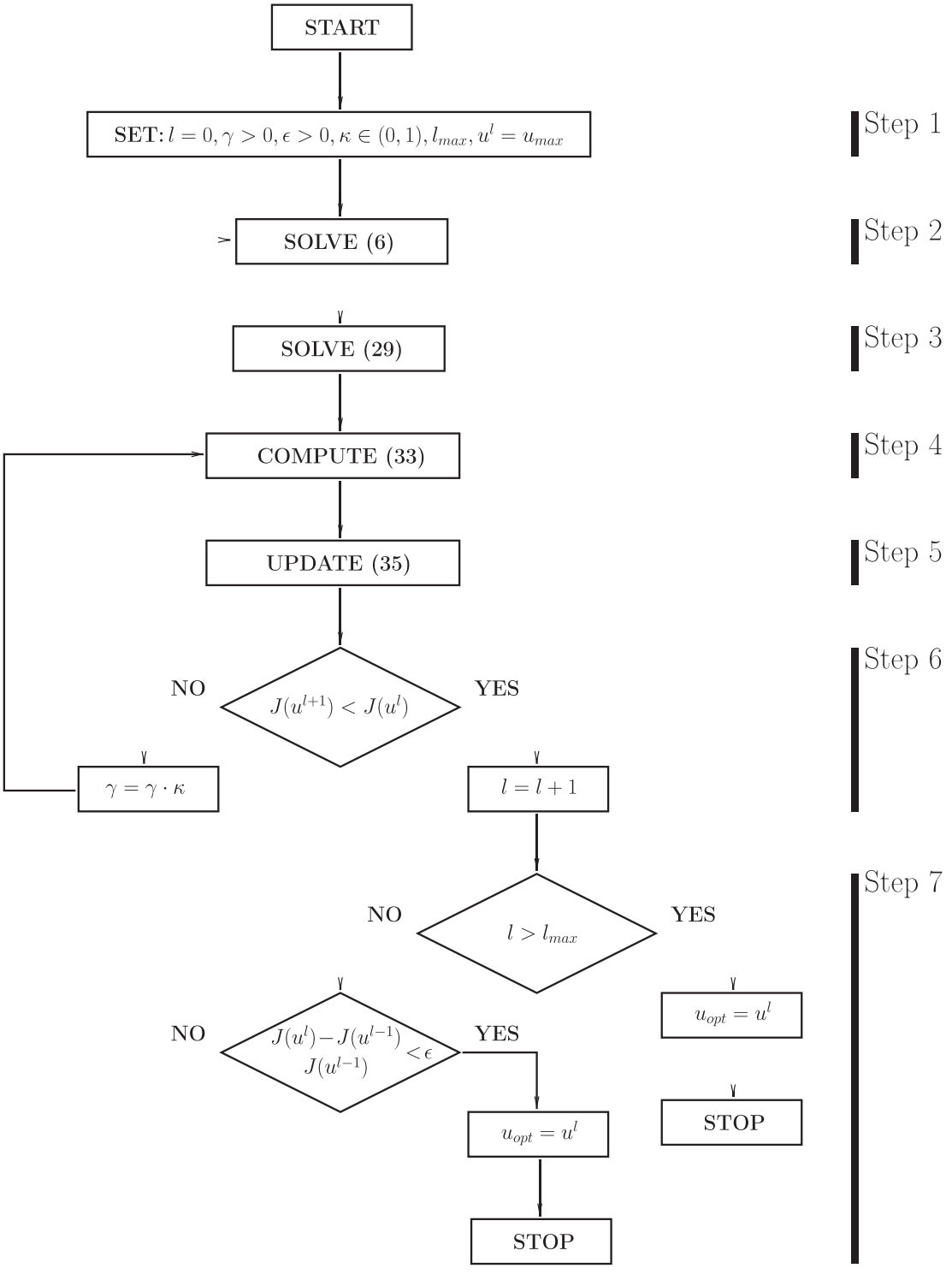

Fig. 16. Scheme of the optimization algorithm presented in Section 6.2.

References

[1] R.A. Ibrahim, Overview of mechanics of pipes conveying fluids – part I: fundamental studies, J. Pressure Vessel Technol. 132 (3) (2010), 034001–1–32.
[2] M.P. Païdoussis, The canonical problem of the fluid-conveying pipe and radiation of the knowledge gained to other dynamics problems across Applied Mechanics, J. Sound Vib. 310 (3) (2008) 462–492.
[3] I. Elishakoff, Controversy associated with the so-called "follower forces": critical overview, Appl. Mech. Rev. 58 (2) (2005) 117–142.
[4] T.B. Benjamin, Dynamics of a system of articulated pipes conveying fluid. I. Theory, Proc. Roy. Soc. Lond. Ser.A Math. Phys. Sci. 261 (1307) (1961) 457–486.
[5] R.W. Gregory, M.P. Païdoussis, Unstable oscillation of tubular cantilevers conveying fluid. II. Experiments, Proc. Roy. Soc. Lond. Ser.A Math. Phys. Sci. 293 (1435) (1966) 528–542.
[6] Y. Sugiyama, Y. Kumagai, T. Kishi, H. Kawagoe, Studies on stability of pipes conveying fluid (the effect of a lumped mass and damping), Bull. JSME 29 (249) (1986) 929–934.
[7] H. Cui, J. Tani, Flutter robust-control of a pipe conveying fluid, Trans. Japan Soc. Mech. Eng. Ser. C 60 (579) (1994) 3789–3793.
[8] J. Tani, Y. Sudani, Active flutter suppresion of a vertical pipe conveying fluid, JSME Int. J. Ser. C Dyn. Control Rob. Des. Manuf. 38 (1) (1995) 55–58.
[9] H. Doki, K. Hiramoto, R. Skelton, Active control of cantilevered pipes conveying fluid with constraints on input energy, J. Fluid Struct. 12 (5) (1998) 615–628.
[10] H. Cui, J. Tani, K. Ohtomo, Robust flutter control of vertical pipe conveying fluid using gyroscopic mechanism, Trans. Japan Soc. Mech. Eng. Ser. C 61 (585) (1995) 1822–1826.
[11] Y.-H. Lin, C.-L. Chu, Active flutter control of a cantilever tube conveying fluid using piezoelectric actuators, J. Sound Vib. 196 (1) (1996) 97–105.
[12] Y.-K. Tsai, Y.-H. Lin, Adaptive modal vibration control of a fluid-conveying cantilever pipe, J. Fluid Struct. 11 (5) (1997) 535–547.
[13] S.A. Fazelzadeh, B. Yazdanpanah, Active flutter suppression of thin-walled cantilever functionally graded piezoelectric pipes conveying fluid, in: 20th Annual International Conference on Mechanical Engineering-ISME2012, School of Mechanical Eng., Shiraz University, Shiraz, Iran, 2012, pp. 1–4.
[14] K. Hiramoto, H. Doki, Simultaneous optimal design of structural and control systems for cantilevered pipes conveying fluid, J. Sound Vib. 274 (3–5) (2004) 685–699.
[15] F. Yigit, Active control of flow-induced vibrations via feedback decoupling, J. Vib. Contr. 14 (4) (2008) 591–608.
[16] D. Pisarski, Optimal control of structures subjected to traveling load, J. Vib. Contr. 24 (7) (2018) 1283–1299.
[17] R. Konowrocki, T. Szolc, M. Michajłow, L. Jankowski, Semi-active reduction of vibrations of periodically oscillating system, in: Active Noise and Vibration Control, Vol. 248 of Solid State Phenomena, Trans Tech Publications, 2016, pp. 111–118.
[18] M. Michajłow, Ł. Jankowski, T. Szolc, R. Konowrocki, Semi-active reduction of vibrations in the mechanical system driven by an electric motor, Optim. Contr. Appl. Meth. 38 (6) (2017) 922–933.
[19] T. Szmidt, D. Pisarski, C. Bajer, B. Dyniewicz, Double-beam cantilever structure with embedded intelligent damping block: dynamics and control, J. Sound Vib. 401 (2017) 127–138.
[20] D. Pisarski, Decentralized stabilization of semi-active vibrating structures, Mech. Syst. Signal Process. 100 (2018) 694–705.
[21] K.E. Graves, D. Toncich, P.G. Iovenitti, Theoretical comparison of motional and transformer emf device damping efficiency, J. Sound Vib. 233 (3) (2000) 441–453.
[22] A. Tonoli, N. Amati, M. Silvagni, Electromechanical dampers for vibration control of structures and rotors, in: M. Lallart (Ed.), Vibration Control, Sciyo, 2010, pp. 1–32. available from: https://www.intechopen.com/books/vibration-control/electromechanical-dampers-for-vibration-control-of-structures-and-rotors.
[23] T. Szmidt, P. Przybyłowicz, Critical flow velocity in a pipe with electromagnetic actuators, J. Theor. Appl. Mech. 51 (2) (2013) 487–496.
[24] J.-S. Bae, M.K. Kwak, D.J. Inman, Vibration suppression of a cantilever beam using eddy current damper, J. Sound Vib. 284 (3) (2005) 805–824.
[25] D. Karnopp, Permanent magnet linear motors used as variable mechanical dampers for vehicle suspensions, Veh. Syst. Dyn. 18 (4) (1989) 187–200.
[26] Y. Kligerman, O. Gottlieb, Dynamics of a rotating system with a nonlinear eddy-current damper, ASME J. Vib. Acoust. 120 (4) (1998) 848–853.
[27] C.-H. Yau, A. Bajaj, O. Nwokah, Active control of chaotic vibration in a constrained flexible pipe conveying fluid, J. Fluid Struct. 9 (1) (1995) 99–122.
[28] A. Bajaj, P. Sethna, Flow induced bifurcations to three-dimensional oscillatory motions in continuous tubes, SIAM J. Appl. Math. 44 (2) (1984) 270–286.
[29] G.S. Copeland, F.C. Moon, Chaotic flow-induced vibration of a flexible tube with end mass, J. Fluid Struct. 6 (1992) 705–718.
[30] M. Païdoussis, C. Semler, Non-linear dynamics of a fluid-conveying cantilevered pipe with a small mass attached at the free end, Int. J. Non Lin. Mech. 33 (1) (1998) 15–32.
[31] Y. Modarres-Sadeghi, C. Semler, M. Wadham-Gagnon, M. Païdoussis, Dynamics of cantilevered pipes conveying fluid. part 3: three-dimensional dynamics in the presence of an end-mass, J. Fluid Struct. 23 (4) (2007) 589–603.
[32] Y. Modarres-Sadeghi, M.P. Païdoussis, C. Semler, Three-dimensional oscillations of a cantilever pipe conveying fluid, Int. J. Non Lin. Mech. 43 (1) (2008) 18–25.
[33] M.P. Païdoussis, Dynamics of tubular cantilevers conveying fluid, J. Mech. Eng. Sci. 12 (2) (1970) 85–103.
[34] T. Szmidt, P. Przybyłowicz, Critical load and non-linear dynamics of becks column with electromagnetic actuators, Int. J. Non Lin. Mech. 67 (2014) 63–73.
[35] Y. Sugiyama, T. Katayama, E. Kanki, K. Nishino, B. Åkesson, Stabilization of cantilevered flexible structures by means of an internal flowing fluid, J. Fluid Struct. 10 (6) (1996) 653–661.
[36] R.R. Mohler, Natural bilinear control processes, IEEE Trans. Syst. Sci. Cybern. 6 (3) (21970) 192–197.
[37] D. Liberzon, Calculus of Variations and Optimal Control Theory: a Concise Introduction, Princeton University Press, New Jersey, 2012.
[38] R.R. Mohler, Bilinear Control Processes, Academic Press, New York, 1973.